Research in Astronomy and Astrophysics, 22:035001 (9pp), 2022 March https://doi.org/10.1088/1674-4527/ac42bf

The Precision Analysis of the Chinese VLBI Network in Probe Delay Measurement

Ting Li[1,2], Lei Liu[1,3], Wei-Min Zheng[1,3,4], and Juan Zhang[1,3]
[1] Shanghai Astronomical Observatory, Chinese Academy of Sciences, Shanghai 200030, China; zhwm@shao.ac.cn
[2] University of Chinese Academy of Sciences, Beijing 100049, China
[3] Shanghai Key Laboratory of Space Navigation and Positioning Techniques, Shanghai 200030, China
[4] National Basic Public Science Data Center, Beijing 100190, China
Received 2021 October 14; accepted 2021 December 1; published 2022 February 8

Abstract

We propose a Very Long Baseline Interferometry (VLBI) precision evaluation method for probe delay measurement, so as to investigate the error contributions from different components in the Chinese VLBI Network (CVN). This method takes the idea of traditional closure delay analysis for distant radio sources. It focuses on the VLBI closure delay only and therefore excludes the influence of probe orbit determination, which makes it very suitable to evaluate the capability of VLBI probe delay measurement. In this paper, we first introduce the principles of closure delay analysis. Then the statistical results of typical CE5 (Chinese Chang'e 5 lunar exploration mission) and HX1 (Chinese Mars exploration mission) observations are presented, including the comparison of the closure delay precisions between CE5 and HX1 for four closed baseline triangles in CVN. According to the result, we realize that the precision discrepancy between CE5 and HX1 in the closure delay analysis is less than that of residual delay after orbit determination, which reflects the precision level of the VLBI delay measurement.

Key words: Very long baseline interferometers – Astronomy data analysis – Space probes

1. Introduction

Very Long Baseline Interferometry (VLBI), as the technique with the highest angular resolution, has been used in astrophysics (Thompson et al. 2001), astrometry (Ma et al. 1998; Schuh & Behrend 2012) and deep space exploration (Zheng et al. 2014; Liu & Zheng 2020) since the mid-1960 s (Matveyenko et al. 1965). The Chinese VLBI Network (CVN) (Liu & Zheng 2020) consists of five radio telescope stations, including Seshan25 (Sh, 25 m telescope established in 1987), Urumqi (Ur, 26 m telescope established in 1993), Miyun (Bj, 50 m telescope established in 2006), Kunming (Km, 40 m telescope established in 2006) and Tianma (Tm, 65 m telescope established in 2012), together with a data processing center located in Shanghai. The primary missions of the processing center are data receiving and playback, correlation, post processing, and probe orbit determination. Using the VLBI technique combined with the ground-based ranging and Doppler velocity measurement, the precise orbit measurement of lunar probe is achieved. CVN has played an important role in probe tracking in the Chinese lunar exploration mission. Besides that, CVN is undertaking the orbit measurement of the Chinese Mars exploration mission. The accuracy of VLBI orbit determination is continuously improved (Hong et al. 2020).

The whole VLBI tracking task can be divided into two stages. The first stage is delay measurement, which includes raw data correlation and post processing. The purpose of this stage is to obtain the observables of each baseline and scan. The second stage is orbit determination, in which a more accurate orbit is reconstructed by combining a priori orbit with those observables obtained at the first stage. Up to now, the precision evaluation of VLBI system is based on the post-fit residuals of delay after orbit determination, which actually contains errors introduced in both delay measurement and orbit determination stages. The precisions of VLBI delay residuals after the orbit determination of Chinese lunar and Mars probes are listed in Table 1.

The observation of CE5 (Chinese Chang'e 5 lunar exploration mission) and HX1 (Chinese Mars exploration mission) are overlapped in the time from 2020 July to 2021 May. The precision difference of VLBI residual delay can be observed between these two missions: the precision of HX1 is higher than that of CE5. At present, it is difficult to identify specific reasons for this difference in the whole complex observation system. To deal with this issue, we propose a new method to evaluate the delay precision of the VLBI system in the delay measurement stage. It is based on the closure delay standard deviation analysis, which does not depend on the orbit determination process, and therefore separates the error in the delay measurement stage from that of orbit determination. Moreover, based on the closure delay principle, the errors related to the station, such as the effects of station atmosphere, clock and geometry, are canceled out. As a result, it provides an

Table 1
Precisions of VLBI Delay Residuals after the Orbit Determination

Probe Name	Frequency Band	Beacon	Residual Delay Precision (ns)
CE1	S	VLBI	6.2
CE2	S	VLBI	4.9
CE3	X	ΔDOR	0.8
CE4	X	ΔDOR	0.7
CE5	X	ΔDOR	0.4
HX1	X	ΔDOR	0.2

Note. The name in the first column begins with CE represents the probe name in Chinese lunar exploration mission, while HX represents the probe name in Chinese Mars exploration mission.VLBI beacon means the measurement and control downlink signal of probe which include the telemetry signal and ranging and velocity measurement signal. ΔDOR beacon means Delta Differential One-Way Ranging signal.

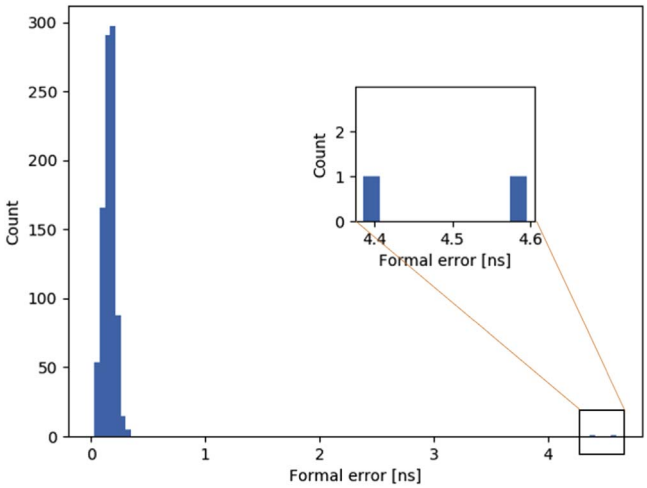

Figure 1. Histogram of formal error.

independent way for the quality assessment of CVN in probe delay measurement stage.

The principle of VLBI closure delay has already been used in astronomy and geodesy. For instance, the closure quantities can reveal the radio source structure information to some extent (Doeleman et al. 2001; Xu et al. 2017; Anderson & Xu 2018). The closure phases and amplitudes have been incorporated in the self-calibration processing of the radio source imaging (Cornwell & Fomalont 1999; Thompson et al. 2001). The differential phase delay closure information can be used to correct delay ambiguity in the differential phase delay calculation of the same beam interferometry (Chen & Liu 2010). In this work, the closure delay method is used to evaluate the precisions of CE5 and HX1 probes in the delay measurement stage. The closure delay precision (the standard deviation) of ΔDOR group delay is calculated. We will demonstrate that the closure delay analysis is suitable for the precision evaluation of CVN probe delay measurement.

In this paper, we first introduce the VLBI closure delay principle in detail. Then we present the results of the closure delay precision analysis of some typical probe observations. Finally, we summarize and give discussions.

2. Closure Delay Principle in VLBI

Imaging that three VLBI stations make up a closed triangle which has three baselines. The closure delay principle is described as that the measured delays and delay rates are summed around these three baselines. The sum of delay and delay rate is called "closure delay" and "closure delay rate". This is a powerful method to test the internal consistency and quality of the data (Whitney 1974). Delay stands for the difference between the arrival time at two stations of the same signal wave front. Delay rate refers to the change rate of delay with respect to time. Given that we have three stations, a, b and c, which form a closed triangle. The arrival times of a certain wave front to the three stations are donated as t_a, t_b and t_c respectively. Then the delay for these three baselines can be expressed as $\tau_{ab} = t_b - t_a$, $\tau_{bc} = t_c - t_b$, and $\tau_{ca} = t_a - t_c$. The closure delay τ_{abc} is defined by

$$\tau_{abc} = \tau_{ab} + \tau_{bc} + \tau_{ca} \quad (1)$$

Theoretically, the closure delay τ_{abc} should be zero if we substitute the delay expressions of τ_{ab}, τ_{bc} and τ_{ca} into formula (1). However, due to the errors introduced during the delay measurement stage, the actual delay of τ_{abc} is not zero. In general, the nonzero closure delay reflects the VLBI delay measurement precision.

In the practical observations, one may be troubled by the fact that the actual time recorded by each station does not correspond to the same wave front of the received signal. Therefore, when calculating the closure delay using the actual delay observables, a correction to the delay observables is needed to make the geometry of a triangle completely close. A detailed discussion about the correction and dedicated equations can be found in the supporting material (Anderson & Xu 2018). A simplified form for the delay correction can be expressed as

$$\tau_{abc} = \tau_{ab} + \tau_{bc} + \tau_{ca} + [\dot{\tau}_{bc} \cdot \tau'_{ab} + \frac{1}{2}\ddot{\tau}_{bc} \cdot \tau'^{2}_{ab}] \quad (2)$$

A prime on a delay symbol indicates only the geometric delay without the station clock offset. A dot and double dots on a delay symbol refer to the first and second order derivative with respect to time (Xu et al. 2017). Conveniently, the time correction has already been considered in the delay processing at Shanghai data processing center.

The biggest advantage of closure delay principle is that during the closure delay calculation, the effects of delay errors related to each station, such as station position errors, station

Table 2
Statistic of CE5 and HX1 Observations for Closed Triangle Bj-Ur-Tm

Date	Probe Name	Freq. Setup (MHz × chan)	Scan Length (s)	FFT Size	Formal Error Average (ns)	Closure Delay Average (ns)	Closure Delay Precision (ns)
20201126	CE5	2 × 16	5	2048	0.199	0.005	0.036
	HX1	8 × 4	30	8192	0.175	−0.019	0.120
20201207	CE5	2 × 16	5	2048	0.382	−0.011	0.372
	HX1	8 × 4	30	8192	0.109	0.027	0.153
20201211	CE5	2 × 16	5	2048	0.167	0.005	0.077
	HX1	8 × 4	30	8192	0.098	−0.003	0.074
20201215	CE5	2 × 16	5	2048	0.239	0.021	0.069
	HX1	8 × 4	30	8192	0.102	−0.009	0.141
20201221	CE5	2 × 16	5	2048	0.127	0.002	0.065
	HX1	8 × 4	30	8192	0.133	0.004	0.046
20210217	CE5	4 × 8	5	2048	0.142	−0.001	0.066
	HX1	8 × 4	30	8192	0.097	0.001	0.016
20210415	CE5	8 × 4	30	8192	0.192	0.040	0.093
	HX1	4 × 8	30	8192	0.101	0.010	0.054
20210512	CE5	8 × 4	30	8192	0.181	−0.016	0.052
	HX1	8 × 4	30	8192	0.196	0.035	0.190

Note. The freq. setup for the third column means the bandwidth of channels and the number of channels.

thermal deformation errors, clock offset errors, cable delay errors, EOP errors, errors from pointing offsets, tropospheric delay errors, ionospheric delay errors, and so on, are canceled out completely. As all these delay errors for each station appear twice with opposite symbols in the calculation of closed triangle delay, the sums of these station related delay terms are zero (Anderson & Xu 2018).

In the closure delay analysis of quasar observation, the nonzero closure errors are mainly from the measurement noise and the source structure effects (Xu 2021). Nevertheless, in probe observation, the probe signal is strong and point-like. So the influence of the source structure could be neglected. We can pay more attention to the analysis of the data handling capability of the complex VLBI delay measurement system. In the actual implementation, the precision of closure delay is estimated with the standard deviation of closure delays.

3. Probe Observations and Closure Results Analysis

We have collected several typical observations of CE5 and HX1 from 2020 November to 2021 May. Here we also listed some important observation parameters such as the channel frequency, the scan length, the FFT size, the triangle formal error, etc. FFT size is set according to the spectral resolution and is proportional to the observation bandwidth. For three baselines, the formal errors, expressed as σ_{ab}, σ_{bc}, σ_{ca}, are derived in the fringe fitting process. Then the formal error for the closed triangle is calculated as $\sigma_{abc} = \sqrt{\sigma_{ab}^2 + \sigma_{bc}^2 + \sigma_{ca}^2}$. Before calculating the closure delay standard deviation, we carry out a preliminary analysis on the triangle formal error. The formal error histogram of one typical probe observation is shown in Figure 1. We can find two small isolated precision bars at around 4.5 ns for this observation, which reflects the abnormal values in the observation. To rule out the effect of poor-quality data, data with the formal error greater than 1 ns has been eliminated while doing closure delay analysis. In the future, this treatment could be applied as a sanity check of the data integrity.

Tables 2 and 3 are the statistics with both CE5 and HX1 observations available within one day. Table 2 lists the information for one closed triangle with three stations Bj, Ur and Tm, marked as Bj-Ur-Tm, while Table 3 lists the information for another closed triangle Km-Ur-Tm. The closure delay precision is estimated as the standard deviation of all closure delays in a given observation. The overviews of the

Table 3
Statistic of CE5 and HX1 Observations for Closed Triangle Km-Ur-Tm

Date	Probe Name	Freq. Setup (MHz × chan)	Scan Length (s)	FFT Size	Formal Error Average (ns)	Closure Delay Average (ns)	Closure Delay Precision (ns)
20201126	CE5	2 × 16	5	2048	0.152	−0.012	0.057
	HX1	8 × 4	30	8912	0.124	−0.035	0.217
20201207	CE5	2 × 16	5	2048	0.374	−0.006	0.365
	HX1	8 × 4	30	8912	0.103	−0.028	0.110
20201211	CE5	2 × 16	5	2048	0.168	0.006	0.070
	HX1	8 × 4	30	8912	0.101	−0.025	0.084
20201215	CE5	2 × 16	5	2048	0.187	0.002	0.070
	HX1	8 × 4	30	8912	0.119	0.030	0.119
20201218	CE5	2 × 16	5	2048	0.714	0.001	0.100
	HX1	8 × 4	30	8912	0.321	−0.010	0.046
20201230	CE5	2 × 16	5	2048	0.192	−0.002	0.044
	HX1	8 × 4	30	8912	0.076	0.012	0.061
20210108	CE5	2 × 16	5	2048	0.222	0.013	0.083
	HX1	8 × 4	30	8912	0.090	0.002	0.063
20210203	CE5	4 × 8	5	2048	0.146	−0.010	0.085
	HX1	8 × 4	30	8912	0.053	−0.001	0.020
20210217	CE5	4 × 8	5	2048	0.126	0.006	0.069
	HX1	8 × 4	30	8912	0.077	0.003	0.012
20210429	CE5	8 × 4	30	8912	0.085	−0.022	0.031
	HX1	8 × 4	30	8912	0.379	−0.016	0.073
20210501	CE5	8 × 4	30	8912	0.209	−0.055	0.146
	HX1	8 × 4	30	8912	0.493	−0.015	0.031
20210503	CE5	8 × 4	30	8912	0.086	−0.005	0.033
	HX1	8 × 4	30	8912	0.078	−0.002	0.019
20210505	CE5	8 × 4	30	8912	0.117	−0.001	0.025
	HX1	8 × 4	30	8912	0.065	−0.005	0.027
20210506	CE5	8 × 4	30	8912	0.112	0.003	0.032
	HX1	8 × 4	30	8912	0.157	0.114	0.365
20210512	CE5	8 × 4	30	8912	0.129	−0.015	0.050
	HX1	8 × 4	30	8912	0.122	−0.009	0.089
20210520	CE5	8 × 4	30	8912	0.093	−0.006	0.053
	HX1	4 × 8	30	8912	0.265	−0.036	0.158

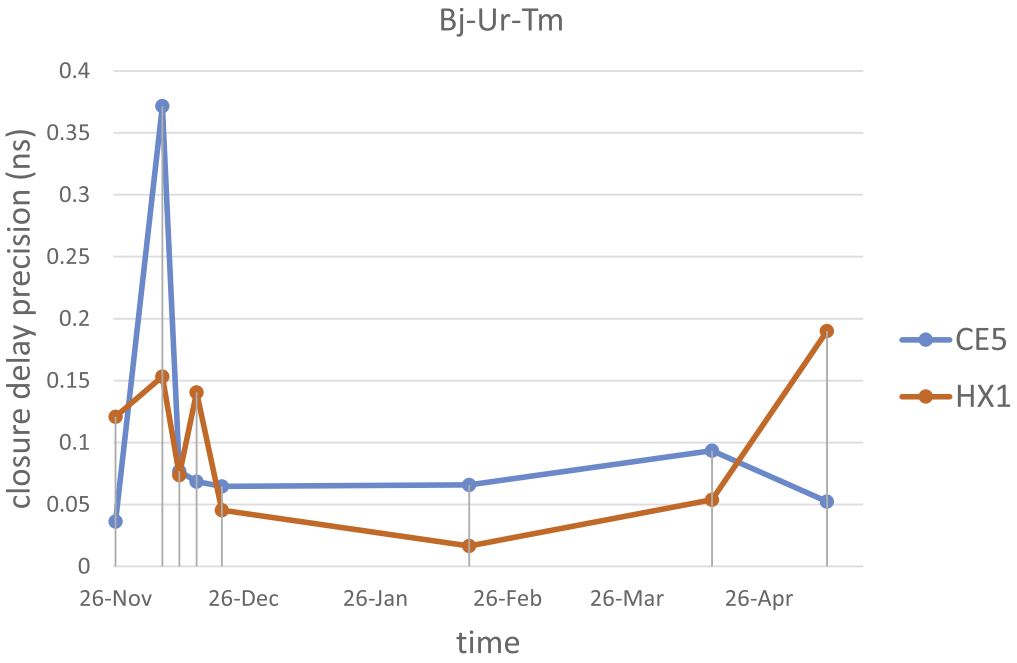

Figure 2. Closure delay precision results of CE5 and HX1 for triangle Bj-Ur-Tm. The observations of two probes were carried out in the same day.

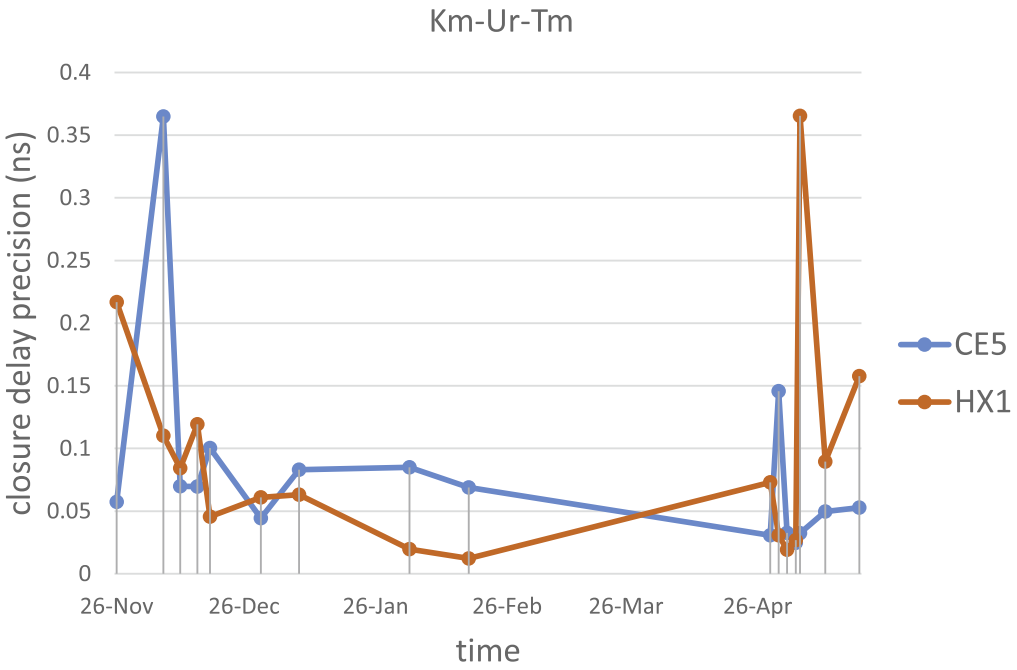

Figure 3. Closure delay precision results of CE5 and HX1 for triangle Km-Ur-Tm. The observations of two probes were carried out in the same day.

closure delay precision results for observations listed in Tables 2 and 3 are shown in Figures 2 and 3, respectively. As illustrated in these two tables and figures, for most observations, the closure delay averages are better than 0.05 ns. Besides that, under the condition of similar formal error, different observation setups yield similar closure delay precision, such as the observation on 2020 December 11. Meanwhile, even though with the same frequency setup and the same scan length, a slight difference appears in the closure delay precisions for some other observations, such as the

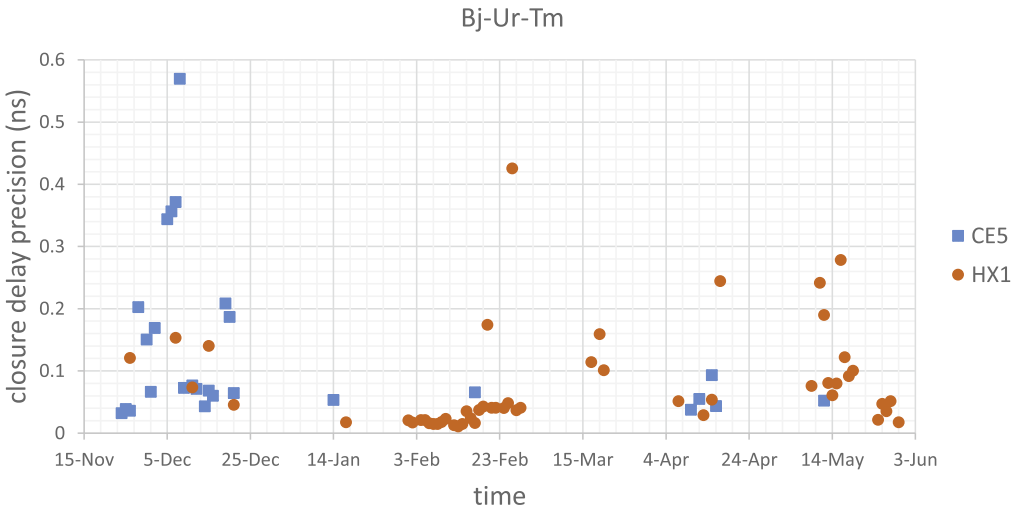

Figure 4. Closure delay precision of all the CE5 and HX1 observations for triangle Bj-Ur-Tm.

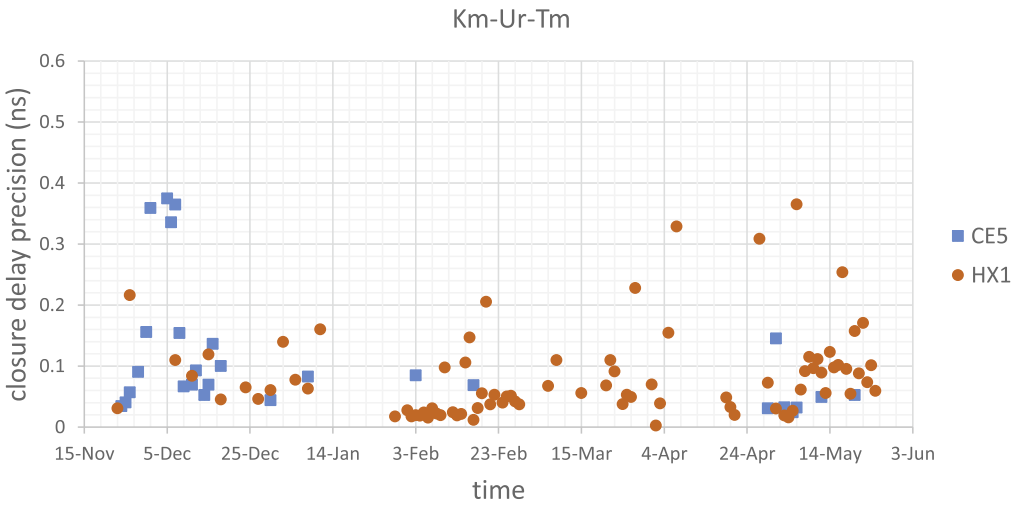

Figure 5. Closure delay precision of all the CE5 and HX1 observations for triangle Km-Ur-Tm.

observation on 2021 May 6. Moreover, for CE5 observations before April 15, the FFT size is set as 2048, while after that is 8192. For HX1 observations, the FFT size is always 8192. Comparing the closure delay precisions among observations after April 15, the difference exists even though all the configurations for frequency, scan length and FFT size are same. This phenomenon suggests that, in CE5 and HX1 observations, the relation between the closure delay precisions and these observation configurations is not prominent.

In Figures 2 and 3, large precision differences between CE5 and HX1 can also be found in December and May. To carry out further investigation, we include more observation data. All CE5 and HX1 observations from the end of 2020 November to the end of May 2021 are collected to calculate the closure delay precisions. Figures 4–7 demonstrate the closure delay precision results of all the CE5 and HX1 observations for closed triangle Bj-Ur-Tm, Km-Ur-Tm, Bj -Km-Ur and Bj-Km-Tm.

To investigate the result in detail, we can divide the whole observation period of these two missions into several phases as illustrated in Figure 8. The CE5 observations were mainly conducted on 2020 November and December. After being launched on November 24, the CE5 probe landed on December 1 and returned to the Earth on December 3 after 3 days' working on the Moon surface. For HX1, before being captured by Mars on February 10, it had a long flight to Mars. Then after orbiting Mars for nearly three months, HX1 landed on May 15. Referring to the closure delay results in Figures 4–7, we can draw some conclusions related to the mission phases. CE5 has a lower delay measurement precision at the beginning of returning phase. The possible explanation is that the orbital

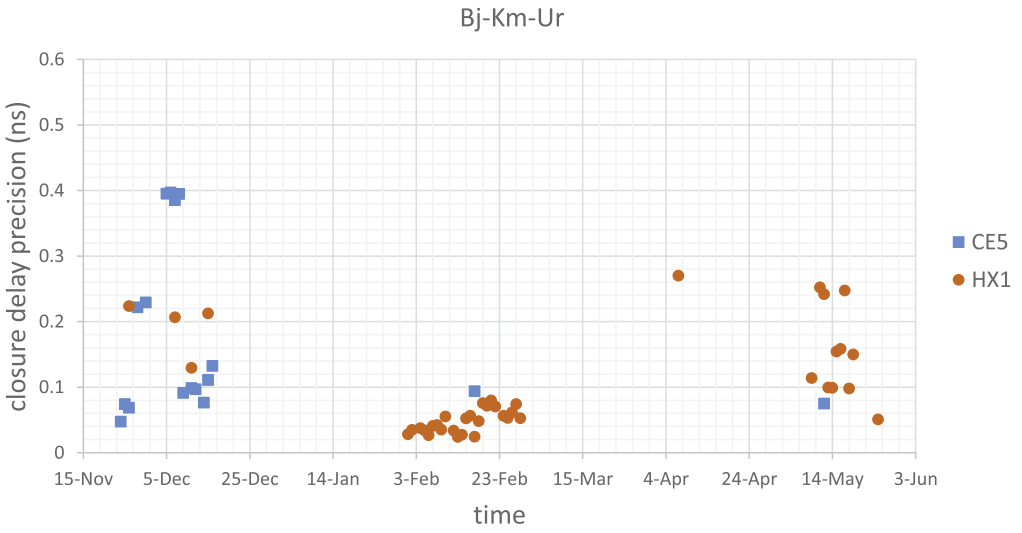

Figure 6. Closure delay precision of all the CE5 and HX1 observations for triangle Bj-Km-Ur.

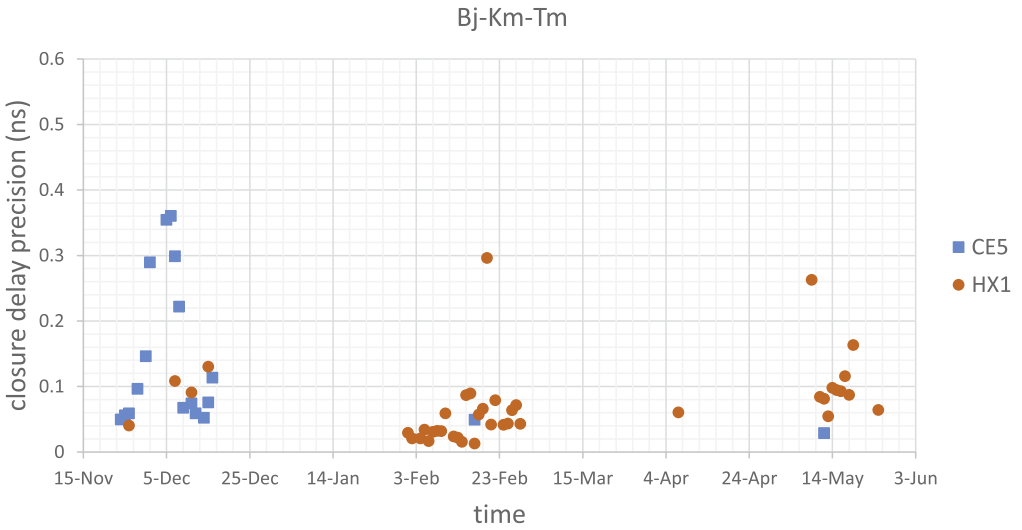

Figure 7. Closure delay precision of all the CE5 and HX1 observations for triangle Bj-Km-Tm.

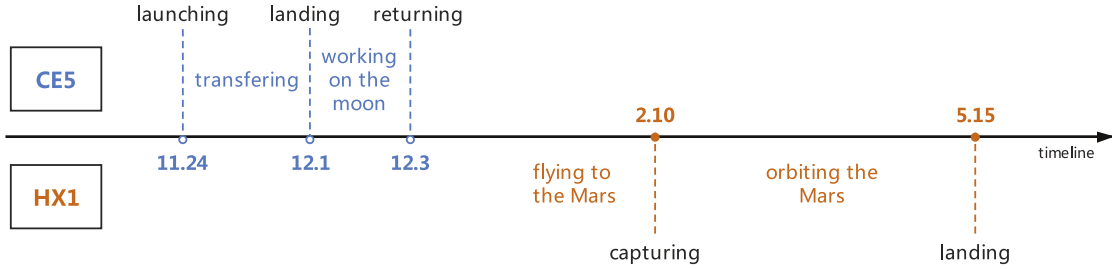

Figure 8. Timeline and key date of CE5 and HX1 mission.

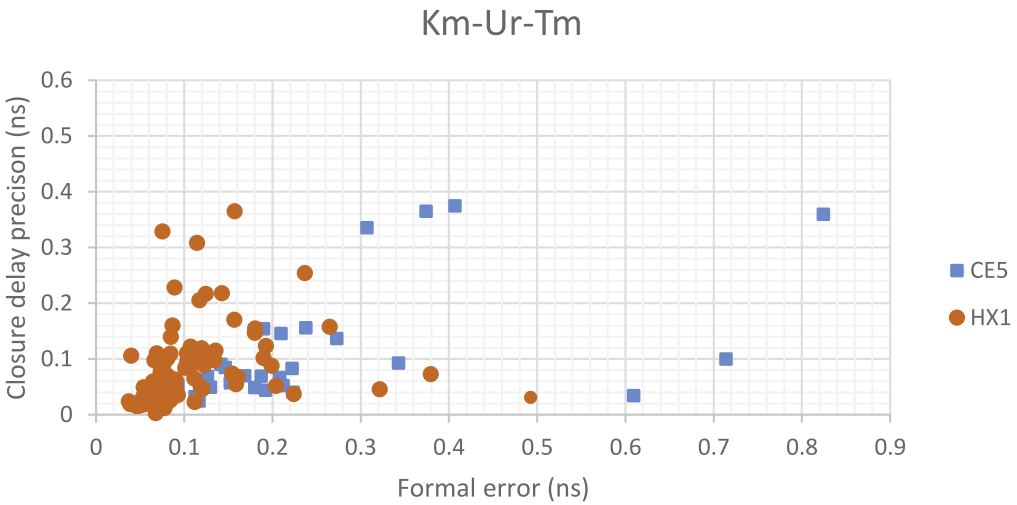

Figure 9. Relation between formal errors and closure delay precisions.

Table 4
Closure Delay Precision Summary

Closed triangle	Bj-Ur-Tm		Km-Ur-Tm		Bj-Km-Ur		Bj-Km-Tm	
Probe name	CE5	HX1	CE5	HX1	CE5	HX1	CE5	HX1
Precision (ns)	0.133	0.076	0.115	0.082	0.176	0.095	0.136	0.072

maneuver and posture adjustment of CE5 conducted frequently which lead to the instability of CE5 signal. For HX1, there is no significant relationship between the mission phases and the closure delay precisions. Moreover, we analyze the relation between the formal error and the closure delay precision for CE5 and HX1. Figure 9 demonstrates the result for triangle Km-Ur-Tm. The relation between the formal error and the closure delay precision is not clearly observed. This may suggest that the error of closure delay is independent of the formal error, which suggests that the closure delay principle is a useful tool to evaluate the quality of VLBI delay measurement.

The mean values of the closure delay precisions for all the observations are presented in Table 4. From the mean values for these four closed triangles, we can find that the closure delay precision of HX1 is higher than that of CE5, which reflects the delay measurement capability in CVN. Nonetheless, the difference between CE5 and HX1 in the delay measurement stage is less than that after orbit determination.

To sum up, from all the closure delay precision results presented in our work, we can find that:

1. As implied by Tables 2 and 3, for most observations, the closure delay averages are better than 0.05 ns. The precision difference is not obvious for observations with both CE5 and HX1 data available within one day. Moreover, the closure delay precisions exhibit no direct relevance to the important observation configurations in CE5 and HX1 tasks.
2. CE5 exhibits a lower closure delay precision at the first few days of the returning phase, which may be due to the instability of the CE5 beacon and the frequent orbit maneuver. For HX1, a clear relationship is not observed between the mission phases and the closure delay precisions.
3. The closure delay precision of HX1 is slightly higher than that of CE5, which illustrates the subtle difference in the delay measurement capability between CE5 and HX1. Nonetheless, the discrepancy in the delay measurement stage is smaller than that after orbit determination.

4. Conclusions and Discussions

The conventional approach for the precision evaluation of the CVN system is based on the post-fit delay residuals after orbit determination. The corresponding result is demonstrated in Table 1, in which a distinct precision difference between the CE5 and HX1 probe is observed. The possible reasons for the difference in delay residuals may be related to the received signal quality of the probe and the complexity of the probe orbit. To investigate the error contributions from different components of CVN probe observations, inspired by the traditional closure delay analysis for distant radio sources, we

propose to apply the closure delay principle to probe delay measurement. Based on the closure delay principle, the effect of orbit determination error is excluded, which makes it possible to focus on only the internal precision of the VLBI delay measurement system.

From the closure delay analysis of the above observations, the precision difference between CE5 and HX1 in the delay measurement stage is better than that after orbit determination. Moreover, we find that the closure delay precisions vary with mission phases and there is no clear relation between the precision and formal error. In addition, we realize that, the statistic of the closure delay precisions in Table 4 demonstrates a slight difference between the two missions. Besides that, based on our current data, the closure delay precision is not so related to the important observation configurations for these two missions. Therefore, the quantity of closure delay is the reflection of the delay precision of the CVN delay measurement system. In general, because the closure delay analysis excludes errors introduced in the orbit determination stage from the whole VLBI system, it provides us a new way to evaluate the precision of the VLBI delay measurement system.

Acknowledgments

This work is supported by the National Natural Science Foundation of China (Grant Nos. 11973011, 11573057, 11903067, U1938114 and U1831137), National Science and Technology Basic Conditions Platform Project "National Basic Science Data Sharing Service Platform" (Grant No. DKA2017-12-02-09), Key Technical Talents of Chinese Academy of Sciences, Shanghai Outstanding Academic Leaders Plan, Lunar Exploration Project and Key Cultivation Projects of Shanghai Astronomical Observatory. We are grateful to all the staff at Bj, Km, Ur, Tm stations and Shanghai data processing center for their operation and support. We would like to thank Prof. Zhihan Qian, Prof. Dongrong Jiang and Dr. Tetsuro Kondo for their kind revisions and suggestions to the paper.

ORCID iDs

Ting Li, https://orcid.org/0000-0003-0042-536X
Lei Liu, https://orcid.org/0000-0002-2920-1880
Wei-Min Zheng, https://orcid.org/0000-0002-8723-8091

References

Anderson, J. M., & Xu, M. H. 2018, JGRB, 123, 10162
Chen, M., & Liu, Q. H. 2010, PABei, 28, 415, (in Chinese)
Cornwell, T., & Fomalont, E. B. 1999, ASP Conf. Ser., Self-Calibration, 180 ed. G. B. Taylor, C. L. Carilli, & R. A. Perley, 187
Doeleman, S. S., Shen, Z. Q., Rogers, A. E. E., et al. 2001, AJ, 121, 2610
Hong, X. Y., Zhang, X. Z., Zheng, W. M., et al. 2020, JDSE, 7, 7, (in Chinese)
Liu, L., & Zheng, W. M. 2020, RAA, 21, 37
Ma, C., Arias, E. F., Eubanks, T. M., et al. 1998, AJ, 116, 516
Matveyenko, L. I., Kardashev, N. S., & Sholomitskii, G. B. 1965, R&QE, 8, 461
Schuh, H., & Behrend, D. 2012, JGeo, 61, 68
Thompson, A. R., Moran, J. M., & Swenson, G. W. 2001, Interferometry and Synthesis in Radio Astronomy (2nd edn; New York: Wiley)
Whitney, A. R. 1974, Precision Geodesy and Astrometry via Very-long-baseline Interferometry, PhD Thesis, Massachusetts Institute of Technology
Xu, M. H., Anderson, J. M., Heinkelmann, R., et al. 2021, JGeod, 95, 51
Xu, M. H., Heinkelmann, R., Anderson, J. M., et al. 2017, JGeod, 91, 767
Zheng, W., Huang, Y., Chen, Z., et al. 2014, in International VLBI Service for Geodesy and Astrometry 2014 General Meeting Proc., VGOS: The New VLBI Network, ed. B. Dirk, D. Karen, & L. A. Kyla (Beijing: Science Press), 466